J|A|C|S
ARTICLES
Published on Web 11/01/2006

Assembly of Triangular Trimetallic Complexes by Triamidophosphine Ligands: Spin-Frustrated Mn^{2+} Plaquettes and Diamagnetic Mg^{2+} Analogues with a Combined Through-Space, Through-Bond Pathway for ^{31}P-^{31}P Spin−Spin Coupling

Jillian A. Hatnean,[†] Ritu Raturi,[†] Julie Lefebvre,[‡] Daniel B. Leznoff,[‡] Gavin Lawes,[§] and Samuel A. Johnson*,[†]

Contribution from the Department of Chemistry & Biochemistry, University of Windsor, Windsor, Ontario, Canada N9B 3P4, Department of Chemistry, Simon Fraser University, British Columbia, Canada V5A 1S6, and Department of Physics, Wayne State University, Detroit, Michigan 48202

Received August 2, 2006; E-mail: sjohnson@uwindsor.ca

Abstract: The reactions of 2 equiv of the ligand precursor $P(CH_2NHPh)_3$ or $P[CH_2NH\text{-}3,5\text{-}(CF_3)_2C_6H_3]_3$ with 3 equiv of $Mn[N(SiMe_3)_2]_2$ provide high-yielding routes to the triangular trinuclear Mn(II) complexes $[P(CH_2NPh)_3]_2Mn_3(THF)_3\cdot 1.5THF$ and $[P(CH_2N\text{-}3,5\text{-}(CF_3)_2C_6H_3)_3]_2Mn_3(THF)_3$. The solid-state structures of these paramagnetic complexes have approximate C_3 symmetry. The magnetic moments from 300 to 1.8 K could be fit as a magnetic Jahn−Teller distorted isosceles triangle. These complexes exhibit spin frustration and possess an $S = {}^1/_2$ ground state, as revealed by a plot of magnetization versus field at 1.8 K; at fields above 3.8 T, the occupation of an excited state with $S = {}^3/_2$ becomes significant. The diamagnetic magnesium analogues were prepared by the reaction of the ligand precursor $P(CH_2NHPh)_3$, $P[CH_2NH\text{-}3,5\text{-}(CF_3)_2C_6H_3]_3$, or $P(CH_2NH\text{-}3,5\text{-}Me_2C_6H_3)_3$ with $^nBu_2Mg$. The solid-state structures of $[P(CH_2NPh)_3]_2Mg_3(THF)_3\cdot 1.5THF$ and $[P(CH_2N\text{-}3,5\text{-}(CF_3)_2C_6H_3)_3]_2Mg_3(THF)_3$ were determined. Solution ^1H NMR spectroscopy was used to demonstrate that the solid-state structures are maintained in solution. The aryl group of the terminal amido donor exhibits slow rotation on the NMR time scale, and this was found to be an electronic effect. Solution $^{31}P\{^1H\}$ NMR spectroscopy revealed an unexpected 15 Hz coupling between phosphorus nuclei in these complexes. Calculations on a model complex using density functional theory demonstrates that this coupling occurs via a combined through-space, through-bond pathway.

Geometric spin frustration[1] in paramagnetic species is of current interest due to its influence on desirable physical properties[2] such as spin-mediated superconductivity.[3] The simplest examples of spin-frustrated species are antiferromagnetically coupled triangular complexes, where the topology of the complex or lattice prevents all pairwise interactions between unpaired spins from being simultaneously satisfied. The most ubiquitous of these are the oxo-centered carboxylate complexes,[4] and interest in the magnetic behavior of trinuclear complexes has recently been renewed.[5] The need for new synthetic approaches to multidimensional assemblies based on spin-frustrated plaquettes has been noted,[6] and a molecular approach[7,8] where the constituent building blocks are robust and retain triangular bonding motifs in the solid state as well as in solution would be advantageous.

The ability of amido ligands to provide bimetallic[9] or larger Mn(II) complexes[10] is known. Our studies have utilized the trianionic triamidophosphine donors $P(CH_2NAr^R)_3$, where Ar^R

† University of Windsor.
‡ Simon Fraser University.
§ Wayne State University.

(1) Toulouse, G. *Commun. Phys.* **1977**, *2*, 115−119.
(2) (a) Greedan, J. E. *J. Mater. Chem.* **2001**, *11*, 37−53. Ramirez, A. P. *MRS Bull.* **2005**, *30*, 447−451. (b) Hopkinson, J.; Coleman, P. *Phys. Rev. Lett.* **2002**, *89*, 267201−267211.
(3) Anderson, P. W. *Science* **1987**, *235*, 1196−1198.
(4) Cannon, R. D.; White, R. P. *Prog. Inorg. Chem.* **1988**, *36*, 195−298.
(5) (a) Cage, B.; Cotton, F. A.; Dalal, N. S.; Hillard, E. A.; Rakvin, B.; Ramsey, C. M. *J. Am. Chem. Soc.* **2003**, *125*, 5270−5271. (b) Berry, J. F.; Cotton, F. A.; Liu, C. Y.; Lu, T.; Murillo, C. A.; Tsukerblat, B. S.; Villagran, D.; Wang, X. *J. Am. Chem. Soc.* **2005**, *127*, 4895−4902. (c) Yoon, J.; Mirica, L. M.; Stack, T. D. P.; Solomon, E. I. *J. Am. Chem. Soc.* **2004**, *126*, 12586−12595. (d) Telfer, S. G.; Kuroda, R.; Lefebvre, J.; Leznoff, D. B. *Inorg. Chem.* **2006**, *45*, 4592−4601.
(6) (a) Harrison, A. *J. Phys.: Condens. Matter* **2004**, *16*, S553−S572. (b) Moulton, B.; Lu, J.; Hajndl, R.; Hariharan, S.; Zaworotko, M. J. *Angew. Chem., Int. Ed.* **2002**, *41*, 2821−2824. (c) Manson, J. L.; Ressouche, E.; Miller, J. S. *Inorg. Chem.* **2000**, *39*, 1135−1141.
(7) Kahn, O. *Molecular Magnetism*; VCH: New York, 1993.
(8) (a) Gatteschi, D. *Adv. Mater. (Weinheim, Fed. Repub. Ger.)* **1994**, *6*, 635−645. (b) Itoh, K., Kinoshita, M., Eds. *Molecular Magnetism: New Magnetic Materials*; Gordon and Breach: Amsterdam, 2000. (c) Miller, J. S., Drillon, M., Eds. *Magnetism: Molecules to Materials*; Wiley-VCH: New York, 2005.
(9) (a) Putzer, M. A.; Pilz, A.; Mueller, U.; Neumueller, B.; Dehnicke, K. *Z. Anorg. Allg. Chem.* **1998**, *624*, 1336−1340. (b) Putzer, M. A.; Neumueller, B.; Behnicke, K.; Magull, J. *Chem. Ber.* **1996**, *129*, 715−719. (c) Belforte, A.; Calderazzo, F.; Englert, U.; Straehle, J.; Wurst, K. *J. Chem. Soc., Dalton Trans.* **1991**, 2419−2427. (d) Chen, H.; Olmstead, M. M.; Pestana, D. C.; Power, P. P. *Inorg. Chem.* **1991**, *30*, 1783−1787. (e) Rouxel, J.; Chevalier, P. *Bull. Soc. Chim. Fr.* **1972**, 111−114. (f) Kennepohl, D. K.; Brooker, S.; Sheldrick, G. M.; Roesky, H. W. *Z. Naturforsch., B: Chem. Sci.* **1992**, *47*, 9−16.

10.1021/ja065597i CCC: $33.50

represents a variety of aryl substituents, to assemble heterobimetallic[11] and polynuclear[12] complexes. Unlike other triamido[13] and amidophosphine[14] ligands, the $P(CH_2NAr^R)_3$ ligands cannot chelate all of their donor atoms to a single metal.[11,12] Herein we show how trimetallic Mn^{2+} spin-frustrated phosphines can be assembled using these ligands, and how their diamagnetic Mg^{2+} analogues maintain their trimetallic structures in solution.

Results and Discussion

Synthesis of Trinuclear Manganese(II) Complexes. The synthesis of complexes of manganese using the ligand precursors $P(CH_2NHPh)_3$ (**1a**) and $P[CH_2NH\text{-}3,5\text{-}(CF_3)_2C_6H_3]_3$ (**1b**) proved to be facile. The reaction of 2 equiv of **1a** with 3 equiv of $Mn[N(SiMe_3)_2]_2$ in THF produced $[P(CH_2NPh)_3]_2Mn_3(THF)_3 \cdot 1.5THF$ (**2a**) as a pale yellow crystalline precipitate over the course of 36 h, as shown in eq 1. Analogously, the reaction of

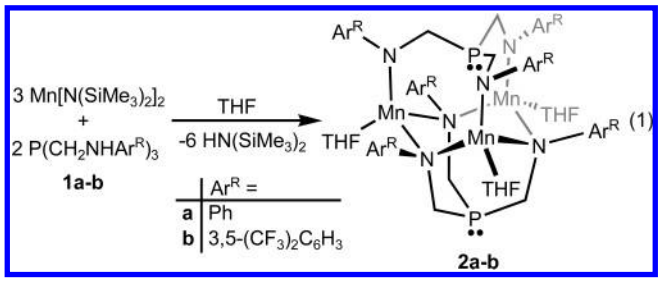

2 equiv of **1b** with 3 equiv of $Mn[N(SiMe_3)_2]_2$ in THF for 72 h produced $[P(CH_2N\text{-}3,5\text{-}(CF_3)_2C_6H_3)_3]_2Mn_3(THF)_3$, which was isolated as a pale yellow crystalline solid by slow evaporation of a concentrated benzene solution. Attempts to react $P[CH_2\text{-}NH\text{-}3,5\text{-}Me_2C_6H_3]_3$ (**1c**) with $Mn[N(SiMe_3)_2]_2$ produced a material which could not be recrystallized, and thus was not further characterized. The 77 K X-band EPR spectra of powder samples of **2a** and **2b** both display a broad resonance at $g = 2.0$, with poorly resolved hyperfine couplings, which is typical for paramagnetic triangular systems.[4,15] Much weaker broad transitions are also observed at 1300 and 2300 G. Although **2a,b** do not have any resolved ^1H or $^{31}P\{^1H\}$ NMR resonances, two broad and shifted ^{19}F resonances are observed for **2b**. Cyclic voltammetry of complexes **2a,b** in THF using $^nBuN^+PF_6^-$ as an electrolyte revealed no reversible oxidation or reduction processes.

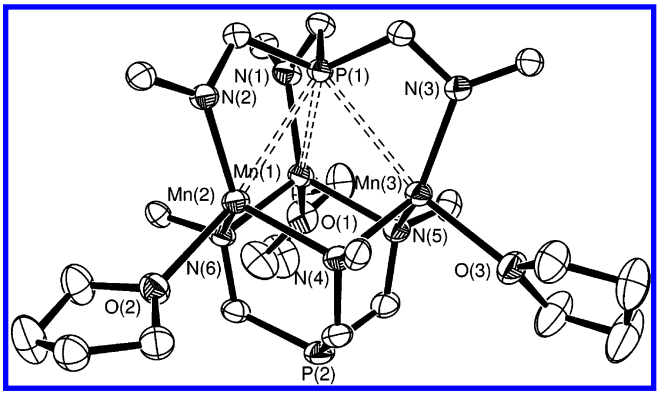

Figure 1. Solid-state molecular structure of **2a** as determined by X-ray crystallography. Only the ipso carbons of the phenyl substituents on nitrogen are shown, and the hydrogen atoms are omitted for clarity. The short contacts between P(1) and the Mn ions are shown as dashed lines. Selected bond lengths or distances (Å): Mn(1)···Mn(2), 3.353(1); Mn(1)−N(1), 2.048(2); Mn(1)−N(6), 2.157(2); Mn(1)−N(5), 2.185(2); Mn(1)−O(1), 2.209(2); Mn(3)···P(1), 2.9122(8); Mn(1)···P(1), 2.978(1); Mn(2)···P(1), 2.976(1). Selected angles in degrees: N(1)−Mn(1)−N(6), 119.38(9); N(1)−Mn(1)−N(5), 127.78(9); N(6)−Mn(1)−N(5), 103.10(9); N(1)−Mn(1)−O(1), 104.25(9); N(6)−Mn(1)−O(1), 105.17(8); N(5)−Mn(1)−O(1), 91.31(8).

The crystals isolated from the synthesis of **2a** proved suitable for X-ray diffraction, and an ORTEP depiction of the solid-state molecular structure is shown in Figure 1. The complex has no crystallographic symmetry, but approximate C_3 symmetry, and contains a trinuclear manganese core supported by two $P(CH_2NPh)_3$ moieties. The average Mn−Mn distance of 3.359(1) Å is approximately twice the van der Waals radius of manganese.

The $P(CH_2NHPh)_3$ ligand moieties in **2a** adopt two different conformations. The lone pair of P(1) is directed toward the inside of the triangle of Mn^{2+} ions, and the amido donors associated with this ligand fragment are each bound terminally to a Mn center, with an average Mn−N distance of 2.060(3) Å. The second ligand fragment has the lone pair of P(2) pointing away from the manganese atoms, and the associated amido donors bridge between Mn atoms, with an average Mn−N distance of 2.169(5) Å. The Mn^{2+} ions attain four-coordinate geometries by binding to one THF molecule each, but they are considerably distorted from a tetrahedral geometry, with the angles to the oxygen donor less than typical tetrahedral angles. The bond angles between the bridging amido donors are also acute, with a N(5)−Mn(1)−N(6) angle of 98.76(10)°, whereas the bond angles between the terminal amido donor and the bridging amides are considerably larger, with N(1)−Mn(1)−N(6) and N(1)−Mn(1)−N(5) angles of 128.26(10) and 120.48(11)°, respectively. The average of the sum of N−Mn−N angles for Mn(1−3) is 351°, which is close to the value expected for a planar arrangement of amido donors. Although the lone pair of P(1) is not properly oriented to bond with a single manganese ion, the distance between P(1) and the Mn^{2+} ions indicates some interaction is probable. The shortest of these is the P(1)−Mn(3) distance of 2.9122(8) Å, which is only ∼5% longer than other comparable P−Mn(II) bonds.[16] For largely ionic bonds, imperfect orbital overlap does not always greatly affect bond strength.[17] The P(1)−Mn(1)−O(1−3) angles range from 160.23-

(10) (a) Alvarez, C. S.; Bond, A. D.; Cave, D.; Mosquera, M. E. G.; Harron, E. A.; Layfield, R. A.; McPartlin, M.; Rawson, J. M.; Wood, P. T.; Wright, D. S. *Chem. Commun.* **2002**, 2980−2981. (b) Alvarez, C. S.; Bashall, A.; Bond, A. D.; Cave, D.; Harron, E. A.; Layfield, R. A.; Mosquera, M. E. G.; McPartlin, M.; Rawson, J. M.; Wood, P. T.; Wright, D. S. *J. Chem. Soc., Dalton Trans.* **2003**, 3002−3008. (c) Crewdson, P.; Gambarotta, S.; Yap, G. P. A.; Thompson, L. K. *Inorg. Chem.* **2003**, *42*, 8579−8584.
(11) Hua, H.; Elsmaili, M.; Johnson, S. *Inorg. Chem.* **2006**, *45*, 7435−7445.
(12) Keen, A. L.; Doster, M.; Han, H.; Johnson, S. A. *Chem. Commun.* **2006**, 1221−1223.
(13) (a) Turculet, L.; Tilley, T. D. *Organometallics* **2002**, *21*, 3961−3972. (b) Jia, L.; Ding, E.; Rheingold, A. L.; Rhatigan, B. *Organometallics* **2000**, *19*, 963−965. (c) Gade, L. H. *Acc. Chem. Res.* **2002**, *35*, 575−582. (d) Gade, L. H. *J. Organomet. Chem.* **2002**, *661*, 85−94.
(14) (a) Fryzuk, M. D. *Can. J. Chem.* **1992**, *70*, 2839−2845. (b) Fryzuk, M. D.; Johnson, S. A.; Rettig, S. J. *J. Am. Chem. Soc.* **1998**, *120*, 11024−11025. (c) Fryzuk, M. D.; Love, J. B.; Rettig, S. J. *Chem. Commun.* **1996**, 2783−2784. (d) Harkins, S. B.; Peters, J. C. *J. Am. Chem. Soc.* **2005**, *127*, 2030−2031. (e) Liang, L.-C.; Lin, J.-M.; Hung, C.-H. *Organometallics* **2003**, *22*, 3007−3009.
(15) (a) Boudalis, A. K.; Sanakis, Y.; Dahan, F.; Hendrich, M.; Tuchagues, J.-P. *Inorg. Chem.* **2006**, *45*, 443−453. (b) Boudalis, A. K.; Sanakis, Y.; Raptopoulou, C. P.; Terzis, A.; Tuchagues, J.-P.; Perlepes, S. P. *Polyhedron* **2005**, *24*, 1540−1548. (c) Kessissoglou, D. P. *Coord. Chem. Rev.* **1999**, *185*−*186*, 837−858.
(16) (a) Godfrey, S. M.; McAuliffe, C. A.; Pritchard, R. G. *J. Chem. Soc., Dalton Trans.* **1993**, 371−375. (b) Hitchcock, P. B.; Lappert, M. F.; Leung, W. P.; Buttrus, N. H. *J. Organomet. Chem.* **1990**, *394*, 57−67.
(17) Bessac, F.; Frenking, G. *Inorg. Chem.* **2006**, *45*, 6956−6964.

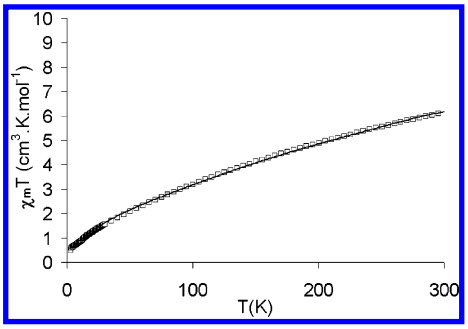

Figure 2. Plot of $\chi_m T$ versus temperature obtained at 10 000 Oe for complex **2b** (□), with the modeled fit shown as a solid line.

(6) to 169.63(6)°, and when these phosphorus−manganese interactions are included, the geometry about the manganese centers is approximately trigonal bipyramidal.

Complex **2b** crystallizes from benzene/hexamethyldisiloxane in both monoclinic and trigonal space groups. In both cases, the connectivity was analogous to that observed for **2a**. Both structures of **2b** suffer from rotational disorder of the CF_3 substituents, and disordered cocrystallized solvent molecules further complicate the trigonal structure. Full details are provided in the Supporting Information.

Magnetic Measurements. The temperature dependence of the molar magnetic susceptibility, χ_m, of **2a** and **2b** was studied over the temperature range of 300−1.8 K. A plot of the product of the susceptibility with the temperature, $\chi_m T$, versus temperature for complex **2b** is shown in Figure 2. At room temperature, $\chi_m T$ is 8.39 $cm^3 \cdot K \cdot mol^{-1}$. This is less than the value of 13.13 $cm^3 \cdot K \cdot mol^{-1}$ expected for three uncoupled Mn(II) centers with five unpaired electrons each, and indicative of antiferromagnetic coupling between the metal centers. The values of $\chi_m T$ steadily decrease down to a minimum of 0.386 $cm^3 \cdot K \cdot mol^{-1}$ at 1.8 K; a spin $^1/_2$ system has an expected value of 0.375 $cm^3 \cdot K \cdot mol^{-1}$. The data for **2a** are provided in the Supporting Information and are similar, with only a slightly lower value of $\chi_m T$ (7.64 $cm^3 \cdot K \cdot mol^{-1}$) at 300 K. Comparable magnetic susceptibilities were obtained for these complexes in solution. Toluene solutions of **2a,b** at 300 K were determined by Evans's method to have $\chi_m T$ values of 6.7 and 7.3 $cm^3 \cdot K \cdot mol^{-1}$, respectively.

Despite the approximate C_3 symmetry of these complexes, the solid-state variable-temperature magnetic susceptibility data are poorly fit by the model predicted from the Heisenberg−Dirac−Van Vleck Hamiltonian for an equilateral triangle, which assumes equal J couplings between all three metal centers. This phenomenon has been the source of considerable debate in the literature,[18] and it has been postulated in related triangular systems that the magnetically degenerate ground state is split by a magnetic Jahn−Teller effect.[19,20] Here we use the static model to fit the observed data to the Hamiltonian appropriate for an isosceles triangle,[21] which uses one value of J to describe the coupling between metal centers labeled 1 and 2 as well as 2 and 3, and a second value, J_{13}, to describe the unique coupling between centers 1 and 3, as shown in eq 2.[21]

$$\hat{\mathbf{H}}_{ex} = -2J[\mathbf{S}_1 \cdot \mathbf{S}_2 + \mathbf{S}_2 \cdot \mathbf{S}_3] - 2J_{13}\mathbf{S}_3 \cdot \mathbf{S}_1 \qquad (2)$$

The energy levels for the states described by S' and S^* for this Hamiltonian are given in eq 3.[4]

$$E(S',S^*) = -J[S'(S'+1) - S^*(S^*+1) - 35/4] - J_{13}[S^*(S^*+1) - 35/2] \qquad (3)$$

Here, $S' = \mathbf{S}_1 + \mathbf{S}_2 + \mathbf{S}_3$ and can take on values from $\pm^{15}/_2$ to $\pm^1/_2$ in integer steps, and $S^* = \mathbf{S}_1 + \mathbf{S}_3$ and can take values from ±5 to 0.

Using this equation, it is possible to calculate the energy levels for any pair of J and J_{13} values. The resultant magnetic susceptibilities can then be determined from the degeneracy of the states, $\Omega(S',S^*)$, provided in the Supporting Information, and their Boltzmann populations at any given temperature, as shown in eq 4.

$$\chi_m = \frac{N\beta^2 g^2}{3kT} \frac{\sum_{S',S^*} S'(S'+1)(2S'+1)\Omega(S',S^*)\, e^{-E(S',S^*)/kT}}{\sum_{S',S^*} (2S'+1)\Omega(S',S^*)\, e^{-E(S',S^*)/kT}} \qquad (4)$$

Here, N is Avogadro's number, β is the Bohr magneton, k is the Boltzmann constant, and the electron proportionality constant g is assumed to be 2.0 for this isotropic Mn(II) system.

The data for **2b** can be fit in this manner using $J = -9.2$ and $J_{13} = -7.0$ cm^{-1}, and the fit is shown as a solid line in Figure 2. An equivalent fit can also be obtained with $J = -7.5$ and $J_{13} = -10.5$ cm^{-1}. The magnetic susceptibility of compound **2a** can be modeled using $J = -11.0$ and $J_{13} = -7.8$ cm^{-1}. Compounds **2a,b** display magnetic coupling that is stronger than that observed in the three examples of related Mn(II) triangular complexes based on carboxylate ligands, whose magnetic properties have been modeled, with reported J values ranging from −0.588 to −2.36 cm^{-1}.[22]

This model predicts a ground-state spin of $^1/_2$, which is characteristic of triangular trimetallic spin-frustrated systems comprised of metals with noninteger spins. This is corroborated by the observed value of $\chi_m T$ at 1.8 K. A plot of the magnetization of **2b** at different field strengths at 1.8 K is shown in Figure 3. The data fit well to the Brillouin function for $S = {}^1/_2$ up to 3 T. At higher fields, the plateau of 1 Nβ predicted from the spin $^1/_2$ Brillouin function, shown as a dashed line in Figure 3, is not observed.

It proved possible to model this deviation from the Brillouin function. As a first approximation, the energy of the states in an applied field, $E(\mathbf{H},S',S^*)$, can be expressed as shown in eq 5.[7]

$$E(\mathbf{H},S',S^*) = E(S',S^*) + S'g\beta\mathbf{H} \qquad (5)$$

An examination of the energy levels predicted from the values of J used to fit the variable-temperature magnetic susceptibility

(18) (a) Uryu, N.; Friedberg, S. A. *Phys. Rev. A* **1965**, *140*, 1803−1811. (b) Sorai, M.; Tachiki, M.; Suga, H.; Seki, S. *J. Phys. Soc. Jpn.* **1971**, *30*, 750−759. (c) Wrobleski, J. T.; Dziobkowski, C. T.; Brown, D. B. *Inorg. Chem.* **1981**, *20*, 684−686. (d) Rakitin, Y. V.; Zhemchuzhnikova, T. A.; Zelentsov, V. V. *Inorg. Chim. Acta* **1977**, *23*, 145−148. (e) Dubicki, L.; Day, P. *Inorg. Chem.* **1972**, *11*, 1868−1875. (f) Jones, D. H.; Sams, J. R.; Thompson, R. C. *J. Chem. Phys.* **1984**, *81*, 440−447. (g) Güdel, H. U. *J. Chem. Phys.* **1985**, *82*, 2510−2511.

(19) For the static model, the anticipated distortion has been calculated to be approximately 0.01 Å: Murao, T. *Phys. Lett. A* **1974**, *49A*, 33−35.

(20) Kahn, O. *Chem. Phys. Lett.* **1997**, *265*, 109−114.

(21) Kambe, K. *J. Phys. Soc. Jpn.* **1950**, *5*, 48−51.

(22) (a) Reynolds, R. A., III; Yu, W. O.; Dunham, W. R.; Coucouvanis, D. *Inorg. Chem.* **1996**, *35*, 2721−2722. (b) Christian, P.; Rajaraman, G.; Harrison, A.; Helliwell, M.; McDouall, J. J. W.; Raftery, J.; Winpenny, R. E. P. *J. Chem. Soc., Dalton Trans.* **2004**, 2550−2555. (c) Lin, W.; Evans, O. R.; Yee, G. T. *J. Solid State Chem.* **2000**, *152*, 152−158.

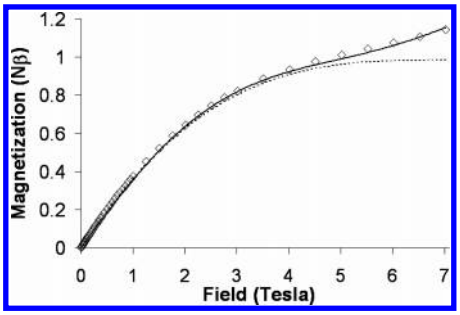

Figure 3. Magnetization versus applied field at 1.8 K for complex **2b** (◇), the Brillouin function for a $S = {}^1/_2$ system (- - -), and the modeled fit (—).

data reveals a low-lying spin $^3/_2$ state 10 cm^{-1} higher in energy than the spin $^1/_2$ ground state in the absence of an applied field. In an applied field, the spin $-^3/_2$ state decreases in energy faster than the spin $^1/_2$ ground state, and its occupancy becomes significant at higher fields. At 1.8 K and in a field of 3.8 T, only 1% of the sample is predicted to be in this spin $-^3/_2$ state, whereas at an applied field of 7 T, 10% of the sample should be in this state. At fields greater than 10 T, the $S = -^3/_2$ state is the predicted ground state. No other states are low enough in energy to have significant populations at 1.8 K under these applied fields. By using the calculated populations of these two states, it is possible to determine a function for the magnetization at any given field in these systems. The modeled field dependency of the magnetization at 1.8 K, determined using $J = -9.24$ and $J_{13} = -7.04$ cm^{-1}, is shown in Figure 3 as a solid line and adequately reproduces the observed data. The modeled fit is very sensitive to both the ratio and values of J and J_{13}.

Based on these analyses, complexes **2a,b** behave as spin-frustrated building blocks with spin $^1/_2$ ground states. The magnetic data can only be suitably fit by assuming that a magnetic Jahn−Teller effect splits the ground-state degeneracy, which yields a low-lying spin $^3/_2$ state as the lowest energy excited state.

Synthesis of Diamagnetic Magnesium Analogues. To serve as useful building blocks for magnetic materials, complexes **2a,b** must maintain their trinuclear structures in solution. To demonstrate that these complexes persist in solution, the Mg(II) analogues were prepared; the ionic radius of Mg(II) is nearly identical to that of Mn(II), and thus similar properties were anticipated. The addition of 3 equiv of ^{n}Bu$_2$Mg to 2 equiv of the ligand precursors **1a**−**c** in tetrahydrofuran provided **3a**−**c**, as shown in eq 6. Analyses of the crude reaction mixtures via ^{1}H and ^{31}P{^{1}H} NMR spectroscopy revealed that no significant side products were formed.

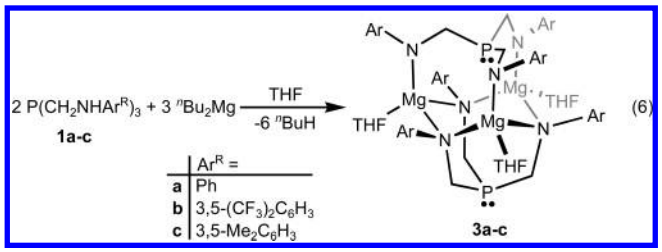

These reactions proceed faster than the formation of **2a,b**, and as a result, X-ray-quality crystals of **3a** could not be obtained directly from the reaction mixture. Instead, the product precipitated as a white powder that is only slightly soluble in benzene or THF. Complex **3a** prepared in this manner analyzes as the trinuclear magnesium complex $[P(CH_2NPh)_3]_2Mg_3(THF)_3 \cdot 1.5THF$ and was isolated in greater than 70% yield by this simple approach. Crystals suitable for X-ray diffraction were obtained from the reaction of $P(CH_2NHPh)_3$ with $(C_5H_5)_2Mg(THF)_2$ in benzene, and sufficiently large crystals formed from the undisturbed reaction mixture.

The solid-state molecular structure of **3a** exhibits the same connectivity as the Mn(II) analogue **2a**. The average Mg−Mg distance of 3.411(1) Å is slightly larger than the average Mn−Mn distance in **2a** of 3.359(1) Å. The average terminal Mg−N bond length of 2.049(3) Å is identical, within error, to the comparable average terminal Mn−N bond length observed for **2a**, whereas the average bridging Mg−N bond distance of 2.146(3) Å is 0.023 Å shorter. These distances are typical of previously structurally characterized Mg amido compounds.[23] The average P(1)−Mg distance is 2.973(1) Å. This is only 0.2−0.3 Å longer than in the few crystallographically characterized magnesium phosphine complexes, which contain Mg−P bond lengths of 2.65−2.77 Å.[24]

Complex **3b** was crystallized from a benzene/hexamethyldisiloxane solution and characterized by X-ray crystallography. Complex **3b** crystallized as two polymorphs, one monoclinic and one hexagonal, both isomorphous to those observed for **2b**. Full details regarding the structures of **3b** are included in the Supporting Information.

The complex $[P(CH_2N\text{-}3,5\text{-}Me_2C_6H_3)_3]_2Mg_3(THF)_3$ (**3c**) was obtained as an analytically pure solid via removal of the THF solvent from the reaction mixture under vacuum; however, the growth of X-ray-quality crystals has so far proven impossible.

Solution Structure. The ^{1}H NMR spectra of **3a**−**c** are consistent with C_{3v}-symmetric species with two ligand environments, and thus they provide verification that the solution structures of these complexes are the same as those determined in the solid state. For each of **3a**−**c**, there are two methylene proton environments associated with each of the two chemically unique triamidophosphine moieties. In the case of complex **3a**, which was isolated cocrystallized with THF, both free and bound THF resonances were observed at room temperature. At higher temperatures these resonances broadened and coalesced, and an activation energy of 57 kJ/mol could be estimated for THF exchange. For complexes **3a** and **3c**, the room-temperature ^{1}H NMR spectra exhibit broad resonances, indicative of slow

(23) (a) Tang, Y.; Zakharov, L. N.; Rheingold, A. L.; Kemp, R. A. *Organometallics* **2005**, *24*, 836−841. (b) Bartlett, R. A.; Olmstead, M. M.; Power, P. P. *Inorg. Chem.* **1994**, *33*, 4800−4803. (c) Bradley, D. C.; Hursthouse, M. B.; Ibrahim, A. A.; Abdul Malik, K. M.; Motevalli, M.; Moseler, R.; Powell, H.; Runnacles, J. D.; Sullivan, A. C. *Polyhedron* **1990**, *9*, 2959−2964. (d) Clegg, W.; Frank, M.; Mulvey, R. E.; O'Neil, P. A. *J. Chem. Soc., Chem. Commun.* **1994**, 97−98. (e) Dozzi, G.; Del Piero, G.; Cesari, M.; Cucinella, S. *J. Organomet. Chem.* **1980**, *190*, 229−236. (f) Duff, A. W.; Hitchcock, P. B.; Lappert, M. F.; Taylor, R. G.; Segal, J. A. *J. Organomet. Chem.* **1985**, *293*, 271−283. (g) Han, R.; Parkin, G. *Organometallics* **1991**, *10*, 1010−1020. (h) Henderson, K. W.; Mulvey, R. E.; Glegg, W.; O'Neil, P. A. *J. Organomet. Chem.* **1992**, *439*, 237−250. (i) Henderson, K. W.; Mulvey, R. E.; Clegg, W.; O'Neil, P. A. *Polyhedron* **1993**, *12*, 2535−2538. (j) Her, T. Y.; Chang, C. C.; Liu, L. K. *Inorg. Chem.* **1992**, *31*, 2291−2294. (k) Holloway, C. E.; Melnik, M. *J. Organomet. Chem.* **1994**, *465*, 1−63. (l) Kennedy, A. R.; Mulvey, R. E.; Schulte, J. H. *Acta Crystallogr., Sect. C: Cryst. Struct. Commun.* **2001**, *C57*, 1288−1289. (m) Magnuson, V. R.; Stucky, G. D. *Inorg. Chem.* **1969**, *8*, 1427−1433. (n) Sebestl, J. L.; Nadasdi, T. T.; Heeg, M. J.; Winter, C. H. *Inorg. Chem.* **1998**, *37*, 1289−1294. (o) Vargas, W.; Englich, U.; Ruhlandt-Senge, K. *Inorg. Chem.* **2002**, *41*, 5602−5608. (p) Westerhausen, M. *Inorg. Chem.* **1991**, *30*, 96−101.

(24) (a) Pape, A.; Lutz, M.; Mueller, G. *Angew. Chem., Int. Ed. Engl.* **1994**, *33*, 2281−2284. (b) Gindelberger, D. E.; Arnold, J. *Inorg. Chem.* **1994**, *33*, 6293−6299.

rotation of one of the two chemically distinct aromatic substituents on the amido groups. For **3b**, this fluxional process is slow enough at room temperature that three ortho proton environments are resolved in the ^{1}H NMR spectrum, in a 2:1:1 ratio, and likewise three fluorine environments are seen in the ^{19}F NMR spectrum. By modeling the variable-temperature ^{1}H NMR spectra, the activation energies for these ring rotations were determined to be 76, 97, and 73 kJ/mol for **3a**−**c**, respectively. This trend is consistent with an electronic rather than a steric barrier to rotation, with the largest activation energy for the electron-withdrawing trifluoromethyl-substituted aryl rings and the lowest barrier for the electron-donating methyl-substituted aromatics. It can be concluded that this fluxional process involves the aromatic substituents on the terminal amido donors, whose lone pair is not involved in σ-bonding, and can thus be delocalized over the aromatic system. This assignment was confirmed by ^{1}H−^{1}H NOESY; the ortho protons of the aromatic substituents associated with the bridging amido exhibit cross-peaks with both sets of ligand methylene protons, whereas the ortho protons of the slowly rotating terminal amido donor substituents exhibit a single cross-peak. These results are consistent with the solid-state structures of **3a**−**c**. There is also evidence for the delocalization of the lone pair over the aromatic substituents from the structural parameters of **3a,b**. In **3a**, the terminal amido−ipso carbon distances N(1)−C(4), N(2)−C(10), and N(3)−C(16) are considerably shorter than the bridging amido−ipso carbon distances N(4)−C(25), N(5)−C(31), and N(6)−C(37); their average distances are 1.379(4) and 1.431(4) Å, respectively, a difference of 0.05 Å. This could be ascribed to partial double bond character in the terminal amido bonds, due to delocalization of the nonbonding amido lone pair over the aromatic substituents,[25] and similar bond lengths have been observed in a related magnesium complex containing both bridging and terminal amido donors.[26]

Through-Space ^{31}P−^{31}P Coupling. Irrespective of temperature, there are two phosphorus environments in the ^{31}P{^{1}H} NMR spectra for each complex, **3a**−**c**, as anticipated from the X-ray structures of **3a** and **3b**. Unexpectedly, the two phosphorus resonances features 15 Hz couplings between phosphorus nuclei; the ^{31}P nuclei are separated by six bonds, two of which are largely ionic in character, and should not readily transmit spin−spin coupling via a Fermi contact term.

Through-space spin−spin coupling is well documented, and most commonly observed with fluorine, although a few examples of ^{31}P−^{31}P through-space coupling are known.[27] The accepted explanation[28] for through-space coupling of nuclear spins is that the overlap of the lone pairs of two adjacent nuclei transmits spin−spin coupling via a Fermi contact term. The coupling is transmitted by a bonding interaction, though no formal bond exists because the antibonding combination of orbitals is also occupied. This mechanism of coupling has been found to display an inverse exponential dependence on the distance between nuclei.[29] Although small couplings have been observed at distances slightly greater than twice the van der Waals radii of the coupled nuclei, coupling constants rapidly drop to zero at greater distances.[30]

From an examination of the structure of **3a**, it is clear that the requirements for traditional through-space spin−spin coupling directly between the phosphorus nuclei are not met. The lone pair of P(1) is directed toward P(2), but the lone pair of P(2) is directed away from P(1). Furthermore, the van der Waals radius of phosphorus is 1.8 Å, and the 5.298 Å distance between P(1) and P(2) is nearly 3 times are large, and approximately 1 Å farther than the maximum predicted distance at which through-space P−P spin−spin coupling should be observable.[30] Although alternate orbital interactions between the phosphorus nuclei could be postulated, such as the interaction of the lone pair on P(1) with a higher lying vacant orbital on P(2), the distance between the nuclei still seems to prohibit any significant direct through-space interaction.

This hypothesis was tested by computational methods using density functional theory and the B3LYP method in Gaussian 03. The simplest relevant model system, two PH_3 molecules arranged in space in an identical manner to the phosphorus nuclei in **3a**, failed to exhibit any significant coupling when studied using the aug-cc-pVTZ basis set available in Gaussian 03. An examination of each of the Fermi contact, paramagnetic spin−orbit, diamagnetic spin−orbit, and spin−dipole contributions to the coupling constant demonstrated that they were all less than 0.1 Hz.

To provide an explanation for the coupling observed in **3a**−**c**, calculations were performed on the model complex $[P(CH_2NH)_3]_2Mg_3$, where the THF molecule has been omitted and the aryl substituent on nitrogen is replaced with a hydrogen atom. The geometry from **3a** was maintained, but with a N−H distance of 1.1 Å. Although this system is far too simplified for us to hope to quantitatively reproduce the experimentally observed coupling, it proved sufficient to gain qualitative insight into the mechanism of spin−spin coupling between phosphorus nuclei. With this simplified model and a minimal 3-21G basis set, a ^{31}P−^{31}P coupling constant of 10.7 Hz was calculated. When the larger aug-cc-pVTZ basis set was utilized for the phosphorus atoms, a 22.1 Hz ^{31}P−^{31}P coupling was calculated for the same geometry; the approximate magnitude of the ^{31}P−^{31}P coupling is well predicted, even with modest basis sets.

The Fermi contact term dominates the coupling for calculations using either basis set; the paramagnetic spin−orbit, diamagnetic spin−orbit, and spin−dipole contributions were all less than ±0.02 Hz. An examination of the molecular orbitals predicted from the DFT calculation using the 3-21G basis set showed that only the HOMO-15 had significant bonding interactions that extended from P(1) to P(2), which is a requirement for a Fermi contact contribution. A depiction of

(25) The shortened bonds could also be construed as being due to the sp^2 versus sp^3 hybridization of the orbitals participating in the N−C bond. Comparison with the methylene N−C bonds, where no delocalization of the lone pair can occur, allows for an approximate contribution to the difference in bond length that can be attributed to the difference in hybridization. The N(1−3)−C(1−3) bonds are on average 1.459(4) Å, whereas the N(4−6)−C(22−24) bond lengths are on average 1.481(4) Å, a difference of only 0.02 Å; this supports the partial double bond character of the terminal amido−ipso carbon bond.

(26) Clegg, W.; Horsburgh, L.; Mulvey, R. E.; Ross, M. J.; Rowlings, R. B.; Wilson, V. *Polyhedron* **1998**, *17*, 1923−1930.

(27) (a) Pastor, S. D.; Shum, S. P.; Rodebaugh, R. K.; Debellis, A. D.; Clarke, F. H. *Helv. Chim. Acta* **1993**, *76*, 900−914. (b) Hierso, J.-C.; Fihri, A.; Ivanov, V. V.; Hanquet, B.; Pirio, N.; Donnadieu, B.; Rebiere, B.; Amardeil, R.; Meunier, P. *J. Am. Chem. Soc.* **2004**, *126*, 11077−11087. (c) Kaupp, M.; Patrakov, A.; Reviakine, R.; Malkina, O. L. *Chem.−Eur. J.* **2005**, *11*, 2773−2782.

(28) Mallory, F. B. *J. Am. Chem. Soc.* **1973**, *95*, 7747−7752.

(29) Mallory, F. B.; Mallory, C. W.; Butler, K. E.; Lewis, M. B.; Xia, A. Q.; Luzik, E. D., Jr.; Fredenburgh, L. E.; Ramanjulu, M. M.; Van, Q. N.; Francl, M. M.; Freed, D. A.; Wray, C. C.; Hann, C.; Nerz-Stormes, M.; Carroll, P. J.; Chirlian, L. E. *J. Am. Chem. Soc.* **2000**, *122*, 4108−4116.

(30) (a) Alkorta, I.; Elguero, J. *Int. J. Mol. Sci.* **2003**, *4*, 64−92. (b) Diz, A. C.; Contreras, R. H.; Natiello, M. A.; Gavarini, H. O. *J. Comput. Chem.* **1985**, *6*, 647−651.

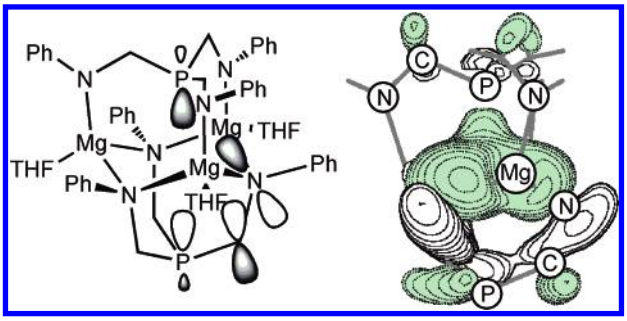

Figure 4. Isosurface of the HOMO-15 in the model complex $[P(CH_2NH)_3]_2Mg_3$, and a simplified depiction of the orbital interactions as they pertain to **3a**.

an isosurface of the orbital generated using Molden[31] is shown in Figure 4. The bonding occurs through space between the lone pair on P(1) and an in-phase combination of an sp^2-hybridized orbitals on each bridging amido donor; however, the coupling is not solely transmitted through space. The nitrogen-based orbital also overlaps with a CH_2 carbon-based p-orbital, which likewise overlaps with an orbital on P(2). A simplification of this interaction, depicted on only one of the three ligand arms, is also shown in Figure 4. The fact that there are three identical coupling pathways presumably plays a role in the magnitude of the coupling constant. At higher energy there is a similar orbital exhibiting antibonding interactions between P(1) and the in-phase combination of sp^2-hybridized orbitals on each bridging amido donor; as expected, no net N−P bonding exists. The contribution of the phosphine lone pair to an orbital that is primarily a component of the ionic amido−magnesium bonds supports a weak bonding interaction between the metals and this phosphine donor.

The observation of $^{31}P-^{31}P$ coupling in these molecules indicates that significant delocalization of σ-bonding occurs over the ligand framework. The transfer of spin information from nitrogen to the phosphorus nuclei in **3a**−**c** suggests that, in complexes **2a**−**c**, significant coupling of electron spins might occur between the Mn_3 fragment and paramagnetic metal centers attached to the phosphine lone pair directed away from the trimetallic core. These complexes could therefore act as spin-frustrated phosphine donors.

Conclusions

The triamidophosphine ligands $P(CH_2NAr^R)_3$, where Ar^R is an aryl substitutent, readily assemble trinuclear clusters with divalent Mn and Mg. The manganese complexes have a degenerate $S = {}^1/_2$ ground state due to spin frustration, with J values that are significantly larger than those for the related trinuclear carboxylate systems. Solution NMR studies show that the diamagnetic magnesium clusters are robust in solution and feature a 15 Hz coupling between ^{31}P nuclei that occurs via a combined through-space, through-bond pathway. This coupling requires extended delocalization of the σ-bonds from the bridging amido donors to the external phosphine. Investigations into the reactivities and use of these clusters as building blocks for molecular magnetic materials are underway. Both the use of the external phosphine as a donor ligand[11] to additional paramagnetic transition metal complexes, and the replacement of the THF donors with donors capable of bridging the trinuclear complexes, should allow for extended structures to be derived from these spin-frustrated building blocks.

Experimental Section

General Procedures. Unless otherwise stated, all manipulations were performed under an inert atmosphere of nitrogen using either standard Schlenk techniques or an MBraun glovebox. Dry, oxygen-free solvents were employed throughout. Anhydrous pentane, toluene, diethyl ether, and THF were purchased from Aldrich, sparged with dinitrogen, and passed through activated alumina under a positive pressure of nitrogen gas; toluene and hexanes were further deoxygenated using Ridox catalyst columns.[32] Deuterated benzene was dried by heating at reflux with sodium/potassium alloy in a sealed vessel under partial pressure and then trap-to-trap distilled and freeze−pump−thaw degassed three times. Deuterated toluene was purified in an analogous manner by heating at reflux over Na. NMR spectra were recorded on a Bruker AMX 300 MHz or 500 MHz spectrometer. All chemical shifts are reported in parts per million , and all coupling constants are in hertz. For $^{19}F\{^1H\}$ NMR spectra, trifluoroacetic acid was used as the external reference at 0.00 ppm. ^1H NMR spectra were referenced to residual protons (C_6D_5H, δ 7.15; C_7D_7H, δ 2.09; $CDHCl_2$, δ 5.32) with respect to tetramethylsilane at δ 0.00. $^{31}P\{^1H\}$ NMR spectra were referenced to external 85% H_3PO_4 at δ 0.0. $^{13}C\{^1H\}$ NMR spectra were referenced to solvent resonances (C_6D_6, δ 128.0; C_7D_8, δ 20.4; CD_2Cl_2, δ 53.8). EPR spectra were collected using an X-band Bruker ESR 300E spectrometer. Unless otherwise noted, magnetizations were measured at 10 000 Oe with a Quantum Design Evercool MPMS-XL7 system. Corrections for the diamagnetic contributions of compounds were made using Pascal's constants. Samples were run both in vacuum-dried gelatin capsules mounted in low-background diamagnetic straws and in a PVC holder specially designed to possess a constant cross-sectional area, with no difference between the two data sets. Cyclic voltammetry was performed using a Bioanalytical Systems 100B/W electrochemical analyzer. Elemental analyses were performed by the Centre for Catalysis and Materials Research (CCMR, Windsor, Ontario, Canada). The compounds tris(hydroxylmethyl)phosphine, aniline, 3,5-dimethylaniline, 3,5-bis(trifluoromethyl)aniline, and 1.0 M dibutylmagnesium in heptane were purchased from Aldrich and used as received. The ligand precursors **1a**−**c**[11] and $Mn[N(SiMe_3)_2]_2$[33] were prepared as previously reported. Bis(cyclopentadienyl)bis(tetrahydrofuran)magnesium was prepared via the literature method,[34] but in our hands it was soluble in hydrocarbon solvents.

Synthesis of $[P(CH_2NPh)_3]_2Mn_3(THF)_3\cdot 1.5THF$ (2a). A solution of $P(CH_2NHC_6H_5)_3$ (500 mg, 1.43 mmol, 2 equiv) and $Mn[N(SiMe_3)_2]_2$ (806 mg, 2.14 mmol, 3 equiv) was dissolved in 5 mL of THF and left undisturbed for 36 h. A crystalline solid containing 1.5 equiv of cocrystallized THF slowly precipitated. The solid was filtered and washed with pentane and 1 mL of THF. The crystalline yellow solid was dried under vacuum (526 mg, 64% yield). A second crop (148 mg, 18%) was obtained by cooling the mother liquor, providing a total yield of 82%. Anal. Calcd for $C_{60}H_{78}Mn_3N_6O_{4.5}P_2$: C, 60.15; H, 6.56; N, 7.01. Found: C, 59.82 H, 6.79; N, 7.08.

Synthesis of $[P(CH_2N\text{-}3,5\text{-}(CF_3)_2C_6H_3)_3]_2Mn_3(THF)_3$ (2b). To a stirred solution of $P(CH_2NH\text{-}3,5\text{-}(CF_3)_2C_6H_3)_3$ (5.0 g, 6.6 mmol, 2 equiv) in 25 mL of THF was added $Mn[N(SiMe_3)_2]_2$ (3.72 g, 9.9 mmol, 3 equiv). The solution was stirred for 72 h. The solvent was evacuated, leaving a tan solid. The product was washed with pentane and dried in vacuo (4.68 g, 75% yield). Pale yellow X-ray-quality crystals containing 1 equiv of benzene were obtained by slow evaporation of an undisturbed solution (2.1 g, 44.9% yield). The cocrytallized benzene could be

(31) Schaftenaar, G. *CAOS/CAMM Center*; The University of Nijmegen: Nijmegen, The Netherlands, 1991.

(32) Pangborn, A. B.; Giardello, M. A.; Grubbs, R. H.; Rosen, R. K.; Timmers, F. J. *Organometallics* **1996**, *15*, 1518−1520.

(33) (a) Andersen, R. A.; Faegri, K., Jr.; Green, J. C.; Haaland, A.; Lappert, M. F.; Leung, W. P.; Rypdal, K. *Inorg. Chem.* **1988**, *27*, 1782−1786. (b) Buerger, H.; Wannagat, U. *Monatsh. Chem.* **1964**, *95*, 1099−1102.

(34) Jaenschke, A.; Paap, J.; Behrens, U. *Organometallics* **2003**, *22*, 1167−1169.

Table 1. Crystallographic Data for Compounds **2a**, **2b**, **3a**, and **3b**

		2b			3b	
	2a	monoclinic	trigonal	3a	monoclinic	trigonal
empirical formula	$C_{60}H_{78}Mn_3N_6O_{4.50}P_2$	$C_{72}H_{60}F_{36}Mn_3N_6O_3P_2$		$C_{69}H_{81}Mg_3N_6O_3P_2$	$C_{72}H_{60}F_{36}Mg_3N_6O_3P_2$	
formula weight	1182.04	1968.02		1177.27	1876.13	
crystal system	triclinic	monoclinic	trigonal	monoclinic	monoclinic	trigonal
a, Å	9.8336(10)	16.2034(17)	24.1780(16)	26.882(4)	16.1671(19)	24.1481(11)
b, Å	13.3050(13)	21.886(2)	24.1780(16)	9.5933(13)	21.732(3)	24.1481(11)
c, Å	22.388(2)	22.723(2)	54.747(8)	25.776(3)	22.771(3)	54.053(5)
α, °	86.3530(10)	90	90	90	90	90
β, °	81.8870(10)	90.1720(10)	90	108.937(2)	90.6540(10)	90
γ, °	84.5170(10)	90	120	90	90	120
volume, Å^3	2882.8(5)	8058.2(15)	27716(5)	6287.4(14)	7999.9(16)	27297(3)
space group	$P\bar{1}$	$P2(1)/c$	$R\bar{3}$	$P2(1)/c$	$P2(1)/c$	$R\bar{3}$
Z	2	4	12	4	4	12
μ (mm^{-1})	0.755	0.636	0.555	0.151	0.212	0.187
temperature (K)	173(2)	143(2)	133(2)	173(2)	133(2)	143(2)
total reflns	32 597	76 431	89 234	58 371	88 776	87 852
no. unique	12 815	14 174	10 839	11 073	18 033	10 690
	[R_{int} = 0.025]	[R_{int} = 0.038]	[R_{int} = 0.051]	[R_{int} = 0.0737]	[R_{int} = 0.0298]	[R_{int} = 0.0449]
residuals: *R*1, wR_2	0.062, 0.156	0.068, 0.146	0.082, 0.176	0.094, 0.140	0.077, 0.175	0.122, 0.313

removed under vacuum. $^{19}F\{^1H\}$ NMR (tol, 282.5 MHz, 20 °C): δ 5.8 (br), 10.1 (br). Anal. Calcd for $C_{66}H_{54}F_{36}Mn_3N_6O_3P_2$: C, 41.94; H, 2.88; N, 4.45. Found: C, 41.71; H, 2.84; N, 4.30.

Synthesis of $[P(CH_2NPh)_3]_2Mg_3(THF)_3\cdot 1.5THF$ (3a). To a stirred solution of $P(CH_2NHPh)_3$ (1.5 g, 4.29 mmol, 2 equiv) in 10 mL of THF was added a 1.0 M heptane solution of $^nBu_2Mg$ (6.44 mL, 6.44 mmol, 3 equiv). The solution was stirred for 4 h at room temperature, over which time a white powder precipitated. The solvent was removed, and the solid was dried under vacuum for 30 min. The product was rinsed with pentane and dried in vacuo (1.616 g, 76.6% yield). Additional product was also recovered from the pentane fraction (246 mg, 11.7% yield) for an overall yield of 88.3%. The microcrystalline sample obtained in this manner contained 1.5 equiv of cocrystallized THF, which could not be removed under vacuum. X-ray-quality crystals were obtained by performing the analogous reaction at room temperature in benzene using $(\eta^5\text{-}C_5H_5)_2Mg(THF)_2$ in lieu of $^nBu_2Mg$. Large colorless crystals containing 2.5 equiv of cocrystallized benzene slowly precipitated from an undisturbed solution; the complex has only slight solubility in benzene. ^1H NMR (CD_2Cl_2, 25 °C, 500.13 MHz): δ 1.5 (m, 12H, $MgOCH_2CH_2$), 1.8 (m, 6H, cocrystallized THF), 3.0 (s, 12H, $MgOCH_2$), 3.68 (m, 6H, cocrystallized THF), 3.75 (d, 6H, PCH_2, J = 6.7 Hz), 3.96 (s, 6H, PCH_2), 5.95 (d, 6H, Ph *o*-H, J = 8.8 Hz), 6.18 (t, 3H, Ph *p*-H, J = 8.8 Hz), 6.7 (t, 3H, Ph *p*-H, J = 8.3 Hz), 6.75 (dd, 6H, Ph *m*-H, J = 7.3 Hz, ^2J = 14.7 Hz), 7.1 (br, 6H, Ph *o*-H and *m*-H), 7.6 (br, 3H, Ph *o*-H). $^{31}P\{^1H\}$ NMR (CD_2Cl_2, 25 °C, 202.46 MHz): δ −22.1 (d, J_{PP} = 15.0 Hz), −32.0 (d, J_{PP} = 15.0 Hz). $^{13}C\{^1H\}$ NMR (C_6D_6, 25 °C, 75.48 MHz): δ 25.1 (s, $MgOCH_2CH_2$), 25.9 (s, cocrystallized THF), 40.9 (s, PCH_2), 42.1 (s, PCH2), 67.5 (s, $MgOCH_2$), 68.0 (s, cocrystallized THF), 113.8 (s, Ph *o*-C), 116.5 (s, Ph *m*-C), 118.5 (s, Ph *p*-C). Anal. Calcd for $C_{60}H_{78}Mg_3N_6O_{4.5}P_2$: C, 65.15; H, 7.11; N, 7.60. Found: C, 64.81; H, 7.10; N, 7.83.

Synthesis of $[P(CH_2N\text{-}3,5\text{-}(CF_3)_2C_6H_3)_3]_2Mg_3(THF)_3$ (3b). To a stirred solution of $P(CH_2NH\text{-}3,5\text{-}(CF_3)_2C_6H_3)_3H_3$ (1.5 g, 1.98 mmol, 2 equiv) in 15 mL of THF was added a 1.0 M heptane solution of $^nBu_2Mg$ (2.97 mL, 2.97 mmol, 3 equiv). The solution was stirred for 2 h at room temperature. The solvent was evacuated, leaving an off-white solid. The product was washed with pentane and dried in vacuo (1.43 g, 80% yield). ^1H NMR (CD_2Cl_2, 25 °C, 300.13 MHz): δ 1.58 (s, 12H, $MgOCH_2CH_2$), 3.08 (s, 12H, $MgOCH_2$), 3.9 (d, 6H, PCH_2, J = 6.4 Hz), 4.12 (d, 6H, PCH_2, J = 3.2 Hz), 6.1 (s, 6H, Ph *o*-H), 6.76 (s, 3H, Ph *p*-H), 7.33 (s, 3H, Ph *o*-H), 7.5 (s, 3H, Ph *p*-H), 7.98 (s, 3H, Ph *o*-H). $^{31}P\{^1H\}$ NMR (CD_2Cl_2, 25 °C, 300 MHz): δ −17.8 (d, J = 14.8 Hz), −33.5 (d, J = 14.6 Hz). $^{13}C\{^1H\}$ NMR (C_6D_6, 25 °C, 75.48 MHz): δ 24.5 (s, $MgOCH_2CH_2$), 46.2 (d, PCH_2, J = 24.2 Hz), 48.1 (d, PCH_2, J = 26.4 Hz), 71.4 (s, $MgOCH_2$), 107 (s, Ph *p*-C), 112 (s, Ph *p*-C), 114 (s, Ph *m*-C), 114.9 (s, Ph *m*-C), 120.4 (s, Ph *o*-C), 122.8 (s, Ph *o*-C), 132 and 134.5 (m, Ph-CF_3, J = 46.11 Hz), 156.3 (s, *ipso*-C), 158.9 (s, *ipso*-C). $^{19}F\{^1H\}$ NMR (CD_2Cl_2, 25 °C, 282.5 MHz): δ 13.89 (s, 9F, Ph-CF_3), 14.06 (s, 18F, Ph-CF_3), 14.18 (s, 9F, Ph-CF_3). Anal. Calcd for $C_{66}H_{54}F_{36}Mg_3N_6O_3P_2$: C, 44.09; H, 3.03; N, 4.67. Found: C, 44.48; H, 3.48; N, 4.28.

Synthesis of $[P(CH_2N\text{-}3,5\text{-}Me_2C_6H_3)_3]_2Mg_3(THF)_3$ (3c). To a stirred solution of $P(CH_2N\text{-}3,5\text{-}Me_2C_6H_3)_3H_3$ (1.0 g, 2.306 mmol, 2 equiv) in 15 mL of THF was added a 1.0 M heptane solution of $^nBu_2Mg$ (3.46, 3.46 mmol, 3 equiv). The solution was stirred for 4 h at room temperature. The solvent was evacuated, leaving a white solid. The product was rinsed with pentane and dried in vacuo (1.08 g, 81.2% yield). ^1H NMR (toluene-d_8, 25 °C, 300.13 MHz): δ 0.92 (s, 12H, $MgOCH_2CH_2$), 2.01 (s, 9H, Ph-CH_3), 2.15 (s, 18H, Ph-CH_3), 2.18 (s, 9H, Ph-CH_3), 3.0 (s, 12H, $MgOCH_2$), 3.8 (s, 6H, PCH_2), 4.25 (s, 6H, PCH_2), 5.85 (s, 6H, Ph *o*-H), 6.2 (s, 3H, Ph *p*-H), 6.42 (s, 3H, Ph *p*-H), 6.63 (br, 3H, Ph *o*-H), 7.8 (br, 3H, Ph *o*-H). $^{31}P\{^1H\}$ NMR (toluene-d_8, 25 °C, 121.5 MHz): δ −22.7 (d, J_{PP} = 15 Hz), −34.3 (d, J_{PP} = 15 Hz). $^{13}C\{^1H\}$ NMR (toluene-d_8, −60 °C, 75.48 MHz): δ 21.4 (s, 3C, Ph-CH_3), 22.2 (s, 6C, Ph-CH_3), 23.1 (s, 3C, Ph-CH_3), 24.7 (s, $MgOCH_2CH_2$), 46.7 (d, PCH_2, J_{PC} = 15.6 Hz), 47.9 (d, PCH_2, J_{PC} = 24.2 Hz), 70.5 (s, $MgOCH_2$), 114.2 (br, Ph *p*-C), 114.5 (s, Ph *p*-C), 119.2 (s, Ph *m*-C), 120.8 (s, Ph *m*-C), 136.5 (s, Ph *o*-C), 139.4 (s, Ph *o*-C), 156.3 (s, Ph *ipso*-C), 159.6 (d, Ph *ipso*-C, J = 24.15 Hz). Anal. Calcd for $C_{66}H_{90}Mg_3N_6O_3P_2$: C, 68.91; H, 7.89; N, 7.31. Found: C, 68.40; H, 7.87; N, 7.31.

X-ray Crystallography. X-ray structures of **2a**, **2b**, **3a**, and **3b** were obtained at low temperature, with each crystal covered in Paratone and placed rapidly into the cold N_2 stream of the Kryo-Flex low-temperature device. Two different polymorphs of **2b** and **3b** were identified. The data were collected using SMART[35] software on a Bruker APEX CCD diffractometer, using a graphite monochromator with Mo Kα radiation (λ = 0.71073 Å). A hemisphere of data was collected using a counting time of 10−30 s per frame. Details of crystal data, data collection, and structure refinement are listed in Table 1. Data reductions were performed using the SAINT[36] software, and the data were corrected for absorption using SADABS.[37] The structures were solved by direct

(35) *SMART, Molecular analysis research tool*; Bruker AXS Inc.: Madison, WI, 2001.
(36) *SAINTPlus, Data reduction and correction program*; Bruker AXS Inc.: Madison, WI, 2001.
(37) *SADABS, An empirical absorption correction program*; Bruker AXS Inc.: Madison, WI, 2001.

methods using SIR97[38] and refined by full-matrix least-squares on F^2, and anisotropic displacement parameters for the non-H atoms, with the exception of some highly disordered solvent molecules, were determined using SHELXL-97[39] and the WinGX[40] software package. The structure of **2a** features a two-fold disordered THF moiety that shows disorder and is refined isotropically, along with a second cocrystallized THF moiety. The monoclinic structure of **3a** features a residual electron density maximum of 1.21 e/Å^3 that is within 0.85 Å of Mg(1). The monoclinic structure of **3b** features a residual electron density maximum of 1.96 e/Å^3 that is within 1.339 Å of F(25), and is associated with a poorly resolved rotational disorder of the CF_3 group. The trigonal structures of **2b** and **3b** suffer from rotational disorder of the CF_3 substituents, disorder of some of the coordinated THF molecules, possible twinning, and disordered cocrystallized solvent molecules that could not be adequately modeled, and they were treated with the SQUEEZE option of PLATON.[41] Hydrogen atoms were excluded on a further disordered cocrystallized benzene molecule in these trigonal structures, as well as on some of the carbons associated with the disordered THF moieties. Thermal ellipsoid plots were produced using ORTEP32.[42]

Calculations. Ab initio DFT calculations were performed using the hybrid functional B3LYP[43] method with the Gaussian 03 package.[44] The basis functions used were the aug-cc-pVTZ and 6-21G set, provided in the Gaussian 03 program.

Acknowledgment is made to the National Sciences and Engineering Research Council (NSERC) of Canada and the Ontario Research and Development Challenge Fund (ORDCF) for their financial support.

Supporting Information Available: Complete ref 44; EPR spectrum for **2a**; $\chi_m T$ versus temperature plot for **2a**; tables of crystallographic data; crystallographic information in CIF format for **2a**, **2b**, **3a**, and **3b**. This material is available free of charge via the Internet at http://pubs.acs.org.

JA065597I

(38) Altomare, A.; Burla, M. C.; Camalli, M.; Cascarano, G. L.; Giacovazzo, C.; Guagliardi, A.; Moliterni, A. G. G.; Polidori, G.; Spagna, R. *J. Appl. Crystallogr.* **1999**, *32*, 115−119.
(39) Sheldrick, G. M. *SHELXL-97*; Universitat Gottingen: Gottingen, 1997.
(40) Farrugia, L. J. *J. Appl. Crystallogr.* **1999**, *32*, 837−838.
(41) Van der Sluis, P.; Spek, A. L. *Acta Crystallogr., Sect. A: Found. Crystallogr.* **1990**, *A46*, 194−201.
(42) Farrugia, L. J. *J. Appl. Crystallogr.* **1997**, *30*, 565.
(43) Becke, A. D. *J. Chem. Phys.* **1993**, *98*, 5648−5652.
(44) Frisch, M. J.; et al. *Gaussian 03*, revision C.01; Gaussian, Inc.: Wallingford, CT, 2004.